

Sand Waves in the Messina Strait, Italy

Authors: Santoro, Vincenza Cinzia, Amore, E., Cavallaro, L., Cozzo, G., and Foti, E.

Source: Journal of Coastal Research, 36(sp1) : 640-653

Published By: Coastal Education and Research Foundation

URL: <https://doi.org/10.2112/1551-5036-36.sp1.640>

BioOne Complete (complete.BioOne.org) is a full-text database of 200 subscribed and open-access titles in the biological, ecological, and environmental sciences published by nonprofit societies, associations, museums, institutions, and presses.

Your use of this PDF, the BioOne Complete website, and all posted and associated content indicates your acceptance of BioOne's Terms of Use, available at www.bioone.org/terms-of-use.

Usage of BioOne Complete content is strictly limited to personal, educational, and non - commercial use. Commercial inquiries or rights and permissions requests should be directed to the individual publisher as copyright holder.

BioOne sees sustainable scholarly publishing as an inherently collaborative enterprise connecting authors, nonprofit publishers, academic institutions, research libraries, and research funders in the common goal of maximizing access to critical research.

Sand Waves in the Messina Strait, Italy

Santoro, Vincenza Cinzia, Amore, E., Cavallaro, L., Cozzo, G., Foti, E.

Department of Civil and Environmental Engineering,
University of Catania
Viale A. Doria, 6 – 95125 Catania, Italy



ABSTRACT

In the present contribution the presence of sand waves in the Messina Strait, Italy, is analysed, on the basis of unpublished data gathered during two different surveys carried out in 1991 and 1992. The study is carried out both from a sedimentological and morphological viewpoint, and in relation to the hydrodynamics in the Strait. Sand waves in two areas are examined: the first one lies just outside the northern part of the Strait, where the flow is rather complex, while the second one lies farther south in the Strait, where the tide characteristics force the flow essentially to oscillate along one direction. As a matter of fact, the dunes are made up with rather coarse sand; therefore, even where current direction varies significantly, only the highest currents are able to mobilise sediment. However, the differences in flow conditions play a significant role on the generation of smaller scale bed-forms (megaripples) in the first area, as obtained from a FFT analysis, and a likely sand bank in the second one.

A morphometric analysis showed that there is not a remarkable variability of these geometric characteristics at constant depth in the two areas. Steepness does not change much as well, and it appears always very low, thus suggesting a likely negligible effect of flow separation on these sand wave morphodynamics.

Time for the examined bed-forms to re-orient has been computed, on the basis of a defect dynamics theory, with the aim of partially investigating the risk for buried cables and pipelines to become exposed. Such time has been estimated as more than one century for both areas, thus implying that it does not play a significant role on problems concerning duct and cable cross design in the Messina Strait.

ADDITIONAL INDEX WORDS: *morphodynamics, sedimentary structures, tidal bed-forms.*

INTRODUCTION

Sand waves are regular patterns in marine non-cohesive bottoms caused by tidal currents, characterised by a wavelength of the order of few hundreds meters and a height of five to ten meters. Besides their intrinsic interest from a geophysical point of view, these sedimentary structures have been widely studied because of their engineering relevance related to their migration speed, which can reach several meters per year. As a consequence, significant changes in bottom morphology can occur, which can cause severe problems to buried pipelines, cables, foundations of offshore structures and to navigation (e.g. Rotterdam Harbour).

In the present contribution the presence of sand waves in the Messina Strait, Italy, is analysed both from a sedimentological and morphological viewpoint, and in relation to the hydrodynamic conditions in the Strait which are rare in the world. Currents higher than 5 m/s have been measured in the Strait, primarily caused by the semidiurnal tide and a phase lag of 180° between the Ionian Sea and the

Tyrrhenian Sea rather than by sea level oscillations. Since a large amount of buried pipelines and cables crosses the Strait, practical interest in studying the characteristics of such sand waves is justified.

Due to the underlying importance, many theoretical studies have been devoted to investigate sand wave formation and migration; however the non-linear interaction between the flow and a cohesionless sandy bottom which causes sand waves to appear is not fully understood. In order to classify the different models, two approaches are usually adopted (WERNER, 1999). The first one is a reductionist approach, whereby the development and behaviour of large-scale features are reduced entirely to their underlying fundamental processes. The second one is a universality approach, whereby the overall characteristics of behaviour and patterns are modelled with the simplest system within a class of systems sharing the same behaviour and characteristics, although composed of very different building blocks.

Among the models which use the first approach, that of FREDSE and DEIGAARD (1993), on the basis of an analogy with a model of dune formation in rivers, proposes a mechanism forced by unidirectional flow, in which the wind wave effects produce only changes in the geometry, precisely on wave height and on wavelength. HULSCHER (1996) presented a model, a 3D extension of the HUTHENANCE's one (1982), based on a stability analysis, which provides the wavelength and crest orientation with respect to the principal tidal current, under the assumption that the ratio between the tidal excursion amplitude and the topographic length scale is small. In 2000 GERKEMA extended the analysis by HULSCHER (1996) by presenting an alternative method of solution, and by further investigating the dependence of the preferred length scale of the sand waves on the parameters in the system. BLONDEAUX *et al.* (1999) formulated a model based on a linear stability analysis in which not only tidal flow is described, but also its interaction with wind waves and steady currents which often coexist and can be thought of as having a large influence on sand wave formation. This model permits the determination of a bottom perturbation of small amplitude, by assuming a small value for the ratio between the amplitude of the tidal wave and the mean water depth, and for the ratio between the mean water depth and the typical length scale of the tidal wave.

Among the models looking for universality, some contributed in providing useful insights by comparing data sets originating from different regions with the aim of identifying the most important factors involved in bed-form generation and control (see, for example, FLEMMING, 2000). However, the one of WERNER and KOCUREK (1997) is, in the authors' opinion, one of the most representative, as it tries to give an interpretation for bed-form patterns by analysing only the dynamics of defects, i.e. the ends of bed-form crests.

In the present paper, a morphometric analysis of unpublished data obtained from different field measurements, taken in 1991 and 1992 respectively in two different areas of the Strait, is presented. A comparison with the theory of FLEMMING (2000) and the one of WERNER and KOCUREK (1997) is then performed.

The paper is organised as follows: in the following section, a geographical, geophysical and lithological description of the study area is given. Then, sand wave characteristics, along with the presence of bed-forms of different length scale, are described. Finally, a discussion on the gathered data and on the above mentioned theories is presented. The paper ends drawing some conclusions and future remarks.

THE STUDY AREA

Geographical and geophysical description

The Messina Strait is a narrow branch of sea, which separates two Italian regions, namely Sicily and Calabria, thus joining the Tyrrhenian and the Ionian Seas (see Figure 1). Its axis is NE-SW oriented in the northern part, which is about 3 km wide, while its southern part, N-S oriented, gradually increases in width, reaching approximately 15 km at a length of about 35 km from the upper end.

From the morphological viewpoint, the sea bottom is highly non-homogeneous (see, among others, SELLI *et al.*, 1979; MONTENAT *et al.*, 1987; COLANTONI, 1987; 1995). In particular, north of the Strait, towards the Tyrrhenian Sea, slopes are mild (generally around 2°-3°) and the sea floor is covered with muddy sediments. Approaching the Strait from the north, in the Scilla Valley region, a narrow U-shaped channel exists, WSW-ENE directed, with depth ranging between 150 and 400 m. The Valley has rough steep flanks (10° northward - 30° southward) and a smooth bottom where sand waves are observed (area 1 in Figure 1), as detected by a survey conducted in 1991 for SNAM. Such a survey was carried out using echo-sounders both from the sea surface and mounted on a ROV, the latter in order to improve the quality of data, particularly on steep slope bottoms. Results of measurements show that these bed-forms extend for approximately 850 m in the W-E direction, verge to N-NW and show megaripples on the current-prone side which verge transversally. It is worth noting that during the survey, an existing pipeline, which in the past had been laid on the sea-bed, was seen to be suspended among two successive crests (i.e. partially floating with respect to the bottom), thus proving the bed-forms had migrated in time. Southward, a smooth gentle-sloped bottom is identified where sand waves are found (area 2 in Figure 1), as revealed by measurements taken in 1988 by Osservatorio Geofisico Sperimentale di Trieste (OGS) for Società Stretto di Messina S.p.A., using a double transducer echo-sounder. In the narrowest branch a Sill exists characterised by a very irregular bathymetry with pinnacles towards the Sicilian bank. Minimum depth in the Sill is 60 m, while the maximum is 115 m within an incised median furrow.

South of the Sill, the U-shaped Messina Valley begins, characterised by a steep slope towards the Sicilian coast (15-40%) and a milder, more regular slope (15-25%) on the Calabrian side. While the flanks exhibit a rough bottom, the floor is relatively flat, covered by sand waves (area 3 in Figure 1) detected during a survey made in 1992 for ENI, using a single beam echo-sounder. At a depth of 500 m the Messina Valley narrows and becomes steeper; here the Messina Canyon begins and rapidly slopes towards the Ionian bathyal plain.

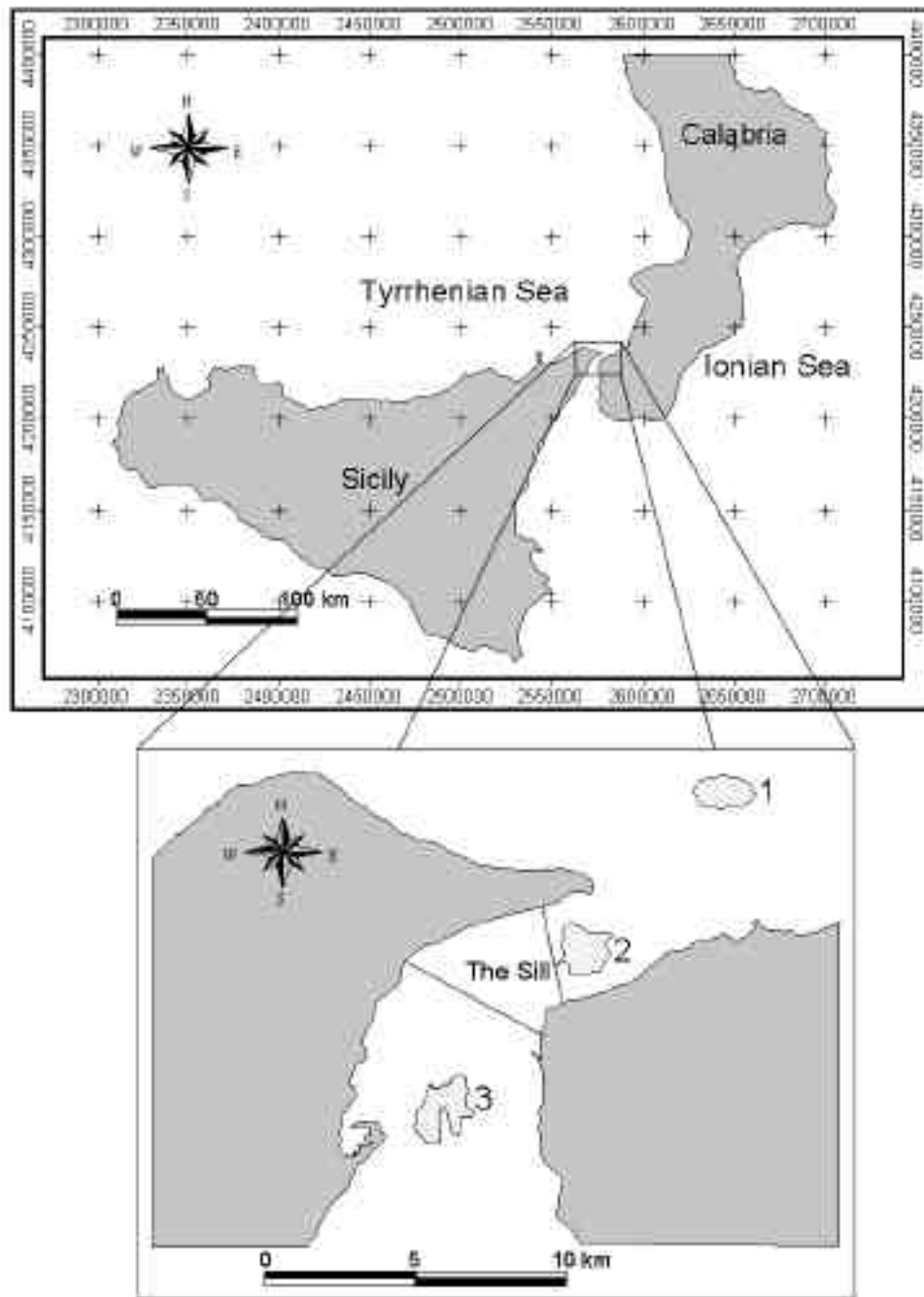


Figure 1. Location of the study area (the coordinates are referred to Gauss-Boaga system). In the zoomed frame, the areas where sand waves were detected during different surveys are shown.

Such variable bathymetry has its key-feature in the Sill, whose origin is of erosive nature but it is probably also controlled by regional tectonics. The Sill, accelerating the flow due to the Venturi effect, is free from depositional processes, being highly subjected to erosion. Small

sediment dunes are partly made up with material eroded from the Sill and, in general, deposited north and south of the Sill, where the flow velocity decreases due to the enlargement of cross-sectional width.

Sediment characteristics

On both sides of the Strait, the coasts are lined with beaches, bands of gravel and sand, which end towards the 100 m bathymetric contour where bare rock is exposed (NESTEROFF and RAWSON, 1987). According to several surveys (among others MONTENAT *et al.*, 1987), bottom deposits can be described, from north to south, as follows.

The Scilla submarine valley is asymmetrically lined by a body of deep coarse sediments. The valley floor is covered with eroded sediments. In the lowermost part of the valley, sand dunes comprise coarse material (sand and gravel). Along the Calabrian slope, bands of bare rock isolate deep sand and gravel from the littoral sand. To the NE of the Strait and submarine valley sediment grade becomes finer.

The Sill is characterised by exposed pinnacles and subjected to current associated erosional processes. Locally, a smooth rocky floor, with patches of pebbly coarse sandstones, is observed.

Symmetrical to the Scilla valley, the Messina valley is characterised in the upper part by a rocky smooth floor with no sediment cover. In the lower part loose sediments with

bioclastic sand, gravel and pebbles form dunes. Between the dune crests, throats are covered with scattered argilloarenaceous mound. In the Messina Canyon, down to 1400 m, the bottom is covered with argilloarenaceous megaripples. In particular, argillosilty sediments alternate with sand and silt, with thickness ranging from one to ten meters.

In summary, from north southward, coarse gravelly sand gives way to finer clayey sand and loam. With regard to the areas where sand waves have been found, Figure 2 shows sediment lithology, as obtained integrating the data of SELLI *et al.* (1979) with the present data gathered during the previously mentioned 1991 SNAM survey.

Sediments reveal heterogeneity even within the same lithological group. Sorting varies from moderate to poor and the skewness from very negative through symmetrical to very positive. This is due to the particular behaviour of the bottom currents in the Messina Strait: where current velocity is higher, and therefore quite coarse sediments can be transported, gravel and sandy gravel have a rather coarse sandy fraction.

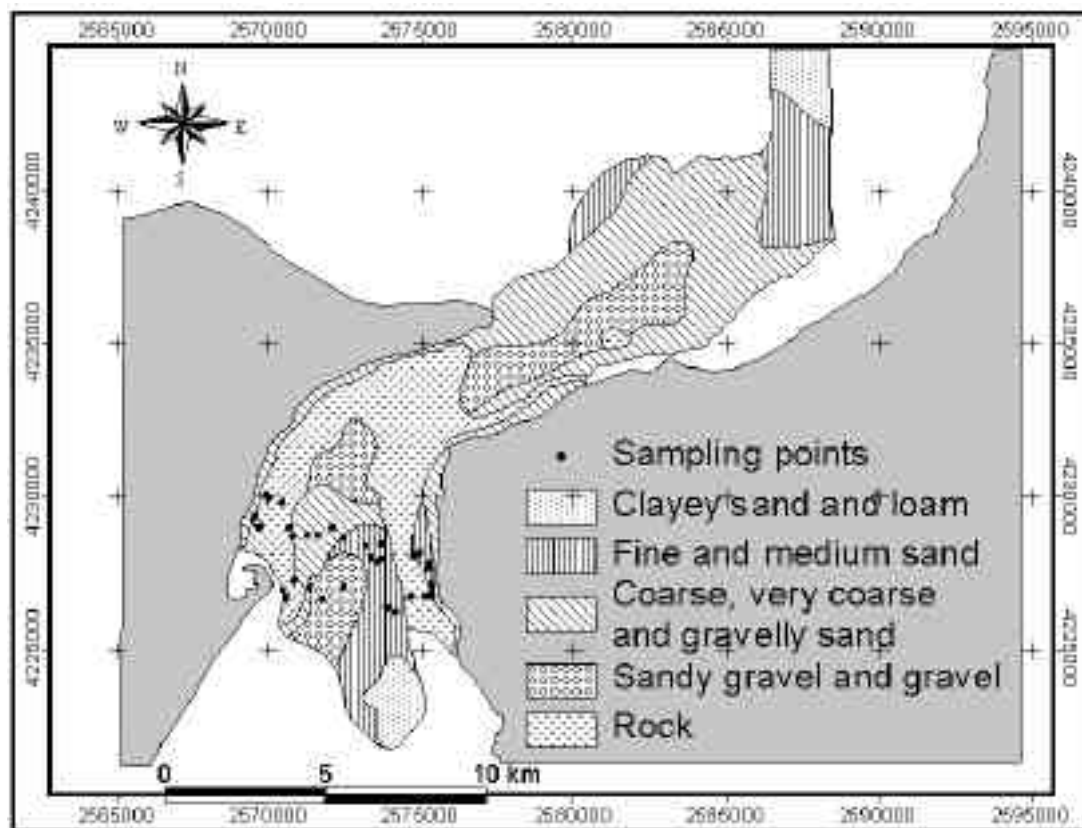


Figure 2. Bottom lithology as obtained integrating the map of SELLI *et al.* (1979) with the present data (the coordinates are referred to Gauss-Boaga system).

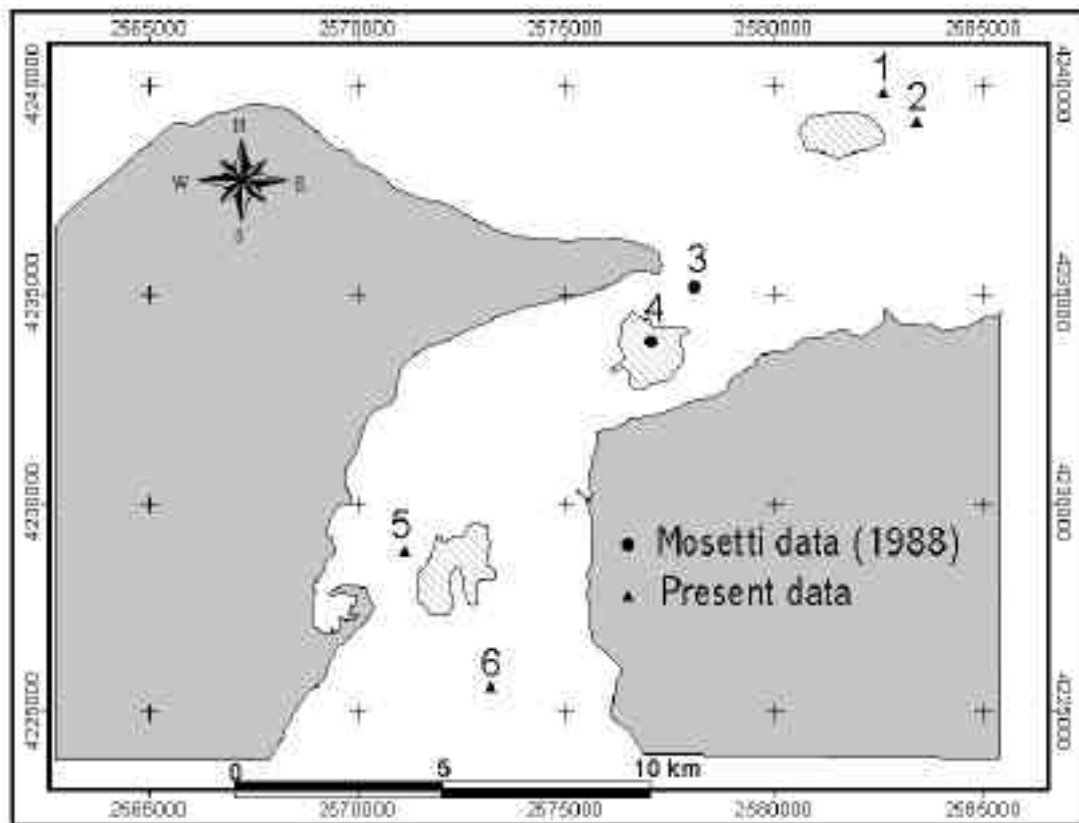


Figure 3. Chosen current survey stations (the coordinates are referred to Gauss-Boaga system).

Hydrodynamic conditions

The Strait is characterised by irregular hydrodynamic conditions. Velocities of several meters per second have been measured, due to the following combined effects: (i) Tyrrhenian and Ionian tides are practically opposite in phase, so that in the Strait sea level oscillations are almost null, while currents are very high. (ii) Density currents present a continuous flow of denser Ionian Sea waters into the Tyrrhenian ones (from south to north), mostly near the bottom of the Strait and in the western side, with a superficial compensation current flow in the opposite way. (iii) The wind causes both strong drift currents at the surface and the upwelling of the waters from the Ionian Sea or from the Tyrrhenian Sea. Moreover, the variable width and the presence of the Sill combine to effect both the current strength and direction in such a way that a non-homogeneous hydrodynamic regime results along the Strait's axis.

As a matter of fact, in the narrowest branch, particle motion is essentially oscillatory along one direction, while north and south of that branch the flow is more complex. In

other words, while in the narrowest part the tidal ellipse can be well described by only few components, elsewhere more harmonics are necessary.

As regard to current measurements, different campaigns have been conducted in the past to better define their characteristics, for sake of easing navigation, designing stable cable anchorage, and even studying the possibility to exploit sea kinetic energy.

In the narrowest part of the Strait, following the first campaign carried out by VERCELLI (1925), few measurements were taken in 1978 (TOMASIN and TOMASINO, 1980) at points close to the surface (-0.1 m and -0.3 m) located slightly west of area 2. According to these data, the M2, S2 and K1 components are the major harmonic constituents of the tide, with maximum total values around 2.30 m/s.

An important survey was made in 1979-80 by Osservatorio Geofisico Sperimentale of Trieste, which provided new and useful information in particular on the tidal currents (MOSETTI, 1988). Indeed, currents were

continuously measured at nine points at different depths. On the Sill, currents as high as 2.00 m/s were measured. From the harmonic analysis, the K1 and M2 components turned out to be the most significant, as a general result. The former ranged roughly between 0.10 and 0.35 m/s, the latter between 0.40 and 1.40 m/s. Direction of such velocities varied slightly with depth and location, but was predominantly aligned with the Strait's axis.

Other different campaigns were conducted respectively in 1982, 1988, besides the above mentioned 1991 and 1992 surveys, to be used for both duct design and preliminary studies regarding a bridge crossing the Strait. This new

body of unpublished data covered almost completely the Strait area, even though most of them were taken close to the surface. In order to use these data for the present morphodynamic study, four stations were selected among them, along with two stations of MOSETTI (1988), these measuring points being at once close to the sand wave areas and to the bottom. Figure 3 shows the location of such points, while Table I reports their characteristics in terms of measuring depth as compared to the bottom one, along with the period of survey.

Figures 4, 5, 6 and 7 show the occurrence of current speed as function of direction (°N) and class of intensity (m/s) in stations 1, 2, 5 and 6 (see Figure 3).

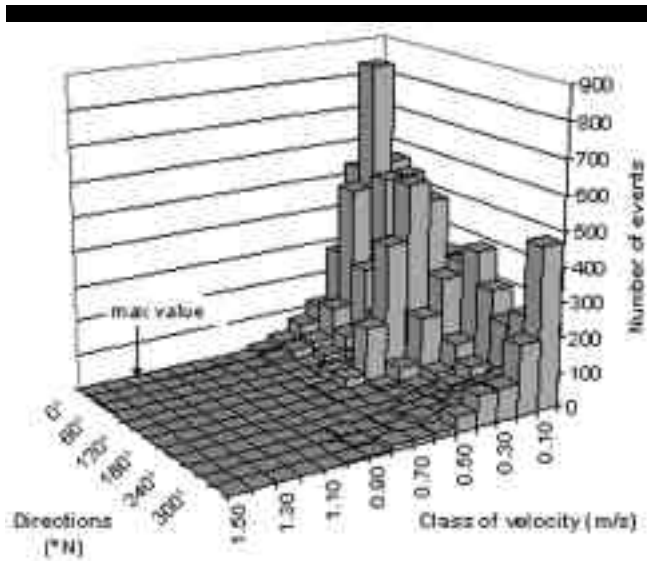


Figure 4. Occurrence of current speed at station 1.

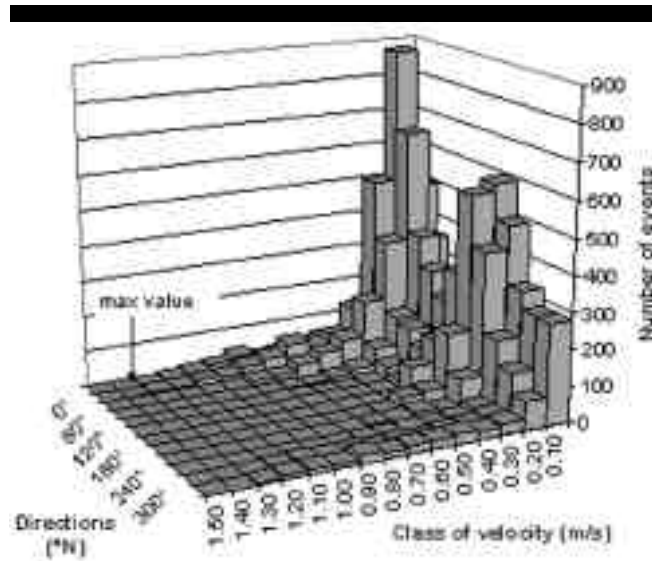


Figure 5. Occurrence of current speed at station 2.

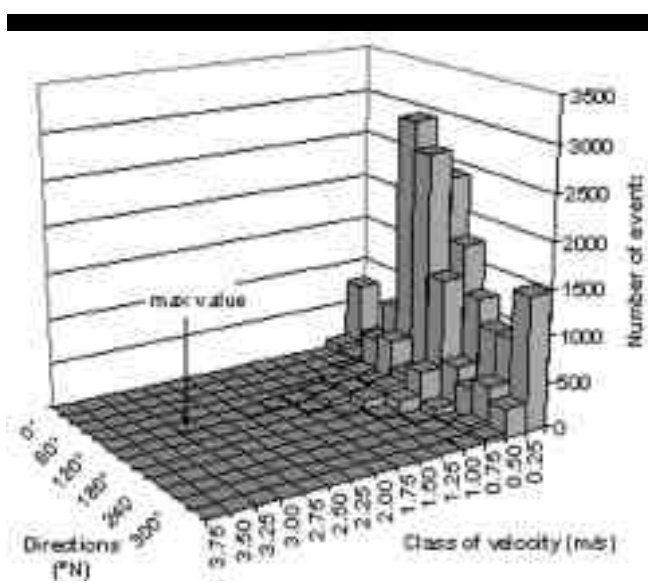


Figure 6. Occurrence of current speed at station 5.

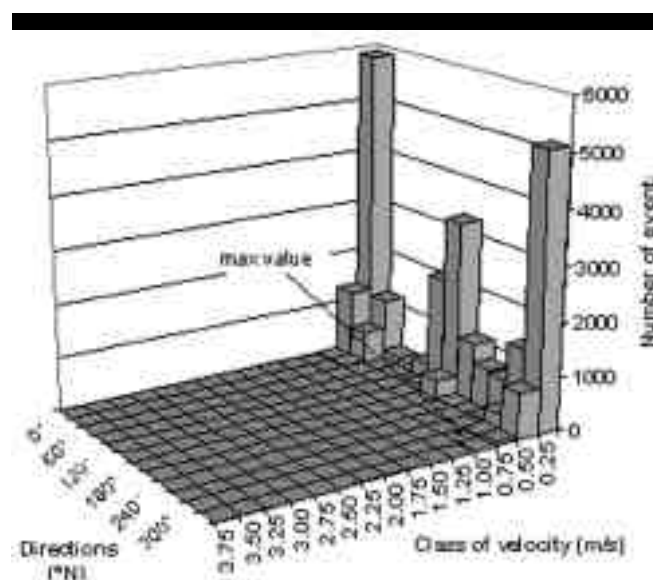


Figure 7. Occurrence of current speed at station 6.

Table I. Main characteristics of the chosen measuring points of bottom currents.

Station	Year	Current meter depth (m)	Bottom (mm/dd/yy)	Period
1	1991	-227	-230	02.02.91-05.01.91
2	1991	-282	-285	03.18.91-06.14.91
3	1979	-222	-226	04.24.80-05.21.80
4	1979	-207	-209	02.27.80-03.26.80
5	1992	-290	-300	01.19.92-07.18.92
6	1992	-340	-350	01.19.92-07.16.92

It is worth pointing out that, even though the sampling interval was 600 s in the four represented stations, the available sets of data are characterised by a class of velocity 0.1 m/s wide at stations 1 and 2 and 0.25 m/s wide at stations 5 and 6.

As regard to maximum measured velocities, both stations 1 and 2, which are located north of the Strait, recorded the highest values, respectively equal to 1.2 and 1.4 m/s, at 0° N. Station 6, which lies inside the Strait south of the Sill, recorded higher maximum velocities (up to 3 m/s at 120° N). At station 5, finally, lower velocities were measured (maximum value being equal to 1 m/s at 120° N). Moreover, while stations 1 and 2 show a similarity in hydrodynamics in terms of both values and their distribution, stations 5 and 6 exhibit a different behaviour of related current. Indeed, recorded currents are different in maximum value and distribution, likely due to the irregular morphology of the bottom in the Strait.

Sand wave analysis

The analysis on sand wave characteristics has been carried out only on areas no. 1 and no. 3 (see Figure 1); data regarding area no. 2 were not close enough to carry out a detailed discussion.

In order to perform a morphometric analysis, all kinds of available data (i.e. cartographic, hydrodynamic and geomorphological) were georeferenced through a Geographical Information System.

The maps of bathymetry thus obtained were used to determine sand wave orientation and to extract a number of bottom profiles, approximately perpendicular to sand wave crests. Figures 8 and 9 respectively display the bathymetric map and the profiles for area no. 1. These profiles were chosen for sake of simplicity, as they all run parallel to each other. Figures 10 and 11 show the same information for area no. 3.

Analysis of profiles was performed by eliminating first the mean slope, which was estimated through a least-squares method. A FFT analysis was then performed on such de-trended profiles; results give interesting information on bed-form characteristics in the two areas, also in terms of mutual comparison. It is worth pointing out that a traditional zero up-crossing method used in oceanography for determining wave characteristics has been here adopted in order to obtain sand wave morphometry.

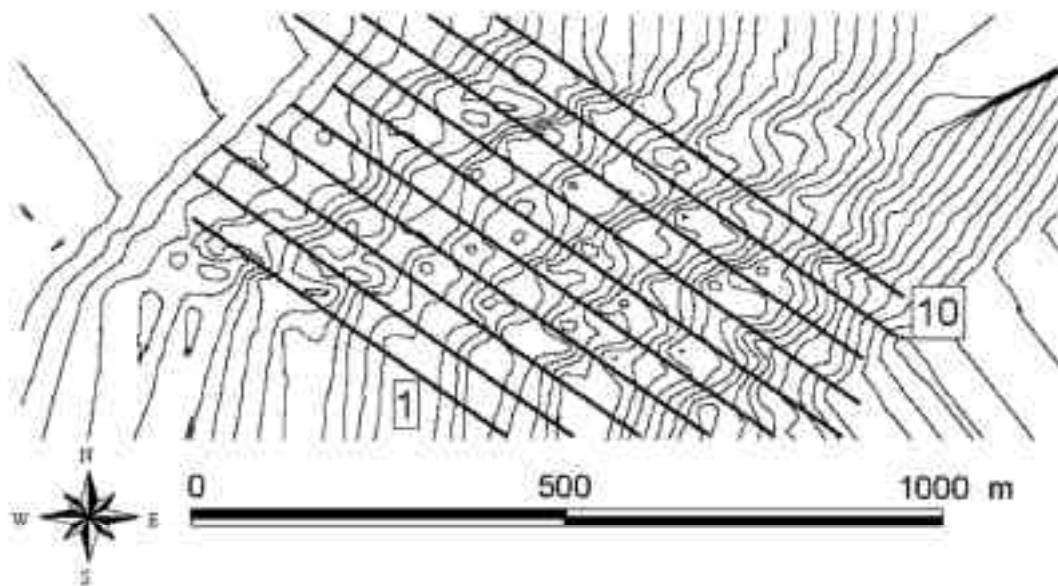


Figure 8. Area no. 1: bathymetry and profile marks.

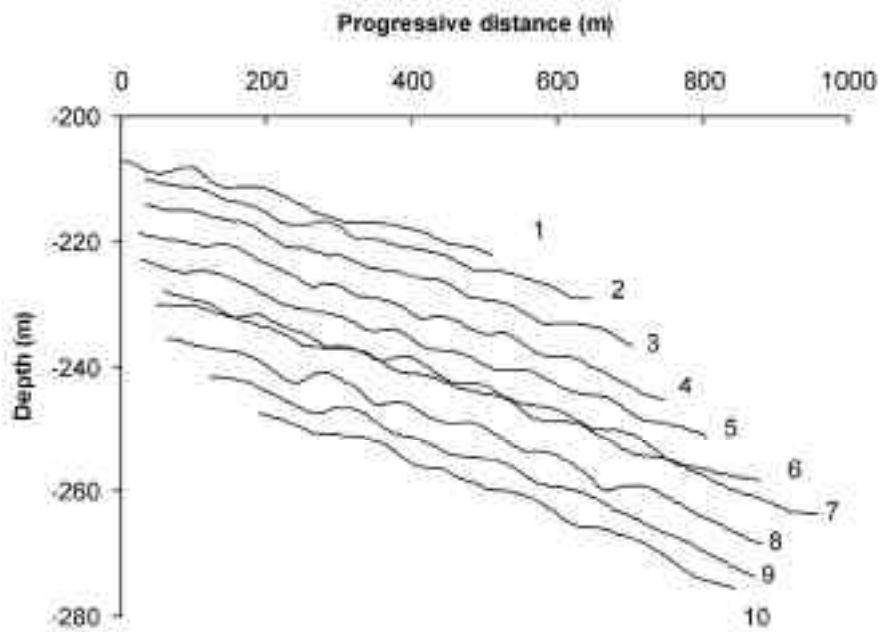


Figure 9. Area no. 1: profiles (starting from profile no. 1, each profile has been offset by 4 m with respect to previous one).

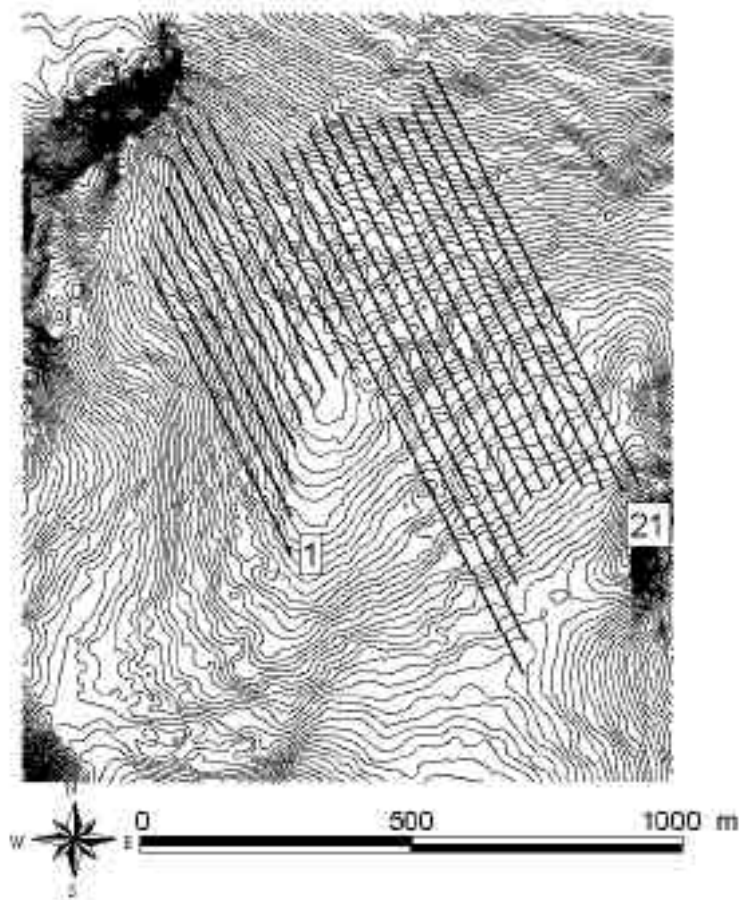


Figure 10. Area no. 3: bathymetry and profile marks.

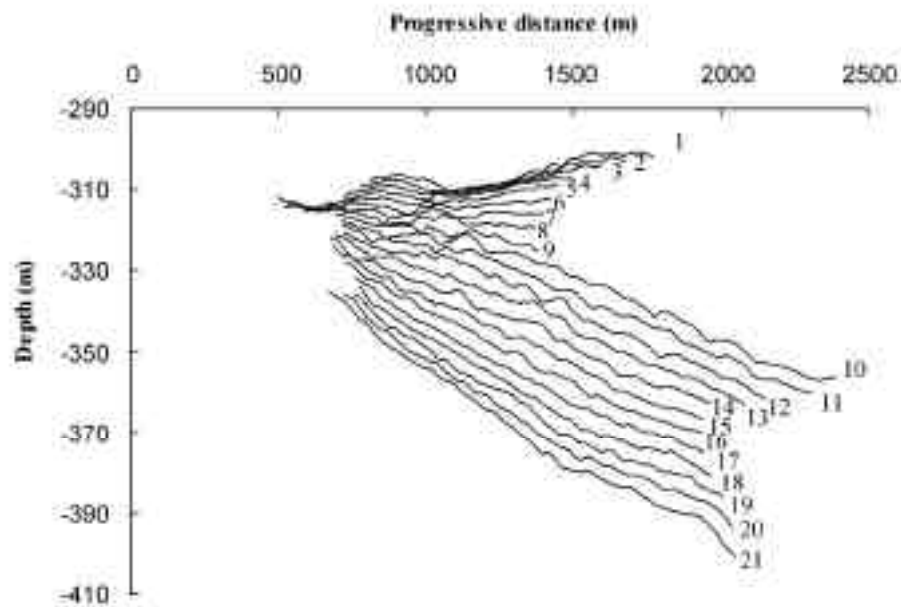


Figure 11. Area no. 3: profiles (starting from profile no. 1, each profile has been offset of 4 m with respect to previous one).

In detail, bottom morphology in area no. 1 shows a variety of patterns forced by the complex hydrodynamics (see Figures 4 and 5), which is responsible for bed-forms with different length scales.

In particular, in the western part of the area, at a depth of -204 m to -209 m, a wide band of megaripples exists. They are characterised by a high asymmetry and their crests advance towards NW. Megaripples reveal various features: some have wavelength ranging from 10 to 30 m and height ranging between 0.5 and 1 m; others have wavelength ranging between 5 and 10 m with a height less than 0.5 m.

In the remaining part of the area there are sand waves with crests advancing in the N-NW direction. Such bed-forms are characterised by a highly 3D structure, being the crests discontinuous and slightly diverging westward. On the current prone side, superposed megaripples exist, verging transversally. From the performed analysis on the profiles marked in Figure 8, sand wave length ranges between 50 and 180 m, while the height ranges between 0.5 and 2.2 m.

A typical profile (in particular no. 3) is shown in Figures 12 and 13, both in the original shape and in the de-trended one; the latter reveals the presence of the above mentioned superposed megaripples.

In area no. 3, the bottom is characterised by sand wave (height $H = 0.5 \div 3.5$ m, wavelength $L = 50 \div 300$ m) and megaripple ($H < 0.50$ m, $L < 50$ m) presence as well. Sand waves advance along the NW direction and are plane on the western side and of barchan type on the eastern one.

Figure 14 shows profile no. 17 as an example of bottom morphology features in area no. 3, while in Figure 15 its de-trended shape is displayed. This latter profile is particularly interesting, as it exhibits a higher order wave-shape, which might reveal the presence of a sand bank. Nevertheless, the length of the available profiles suggests to carefully advance this hypothesis. If true, this could be explained looking at the characteristics of the bottom currents (see Figure 7), which vary little in orientation and could therefore allow large scale bed-forms to develop.

Morphometric characteristics were also determined for range of depths as reported in Table II and Table III for areas no. 1 and no. 3 respectively. In particular, in the first column the range of depth is shown. In the second and third columns the mean height (H_m) and the mean length (L_m) of sand waves are reported respectively. In the last column the steepness ($S=H_m/L_m$) is given.

It is worth pointing out that in each area there is not a remarkable variability of those characteristics. Indeed the maximum scatters between class average and total average values of H_m and L_m are 28% and 26% respectively in area no. 1, while they are 48% and 58% respectively in area no. 3. Moreover, as regard the steepness, it appears always close to 0.01, thus suggesting a likely negligible effect of flow separation on the examined sand wave morphodynamics.

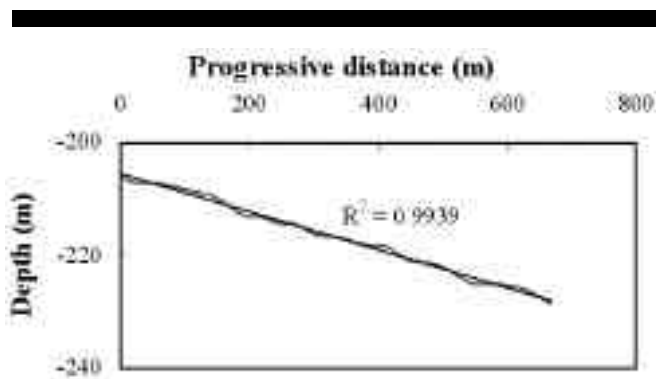


Figure 12. Profile no. 3 in area no. 1: original data and mean slope profile.

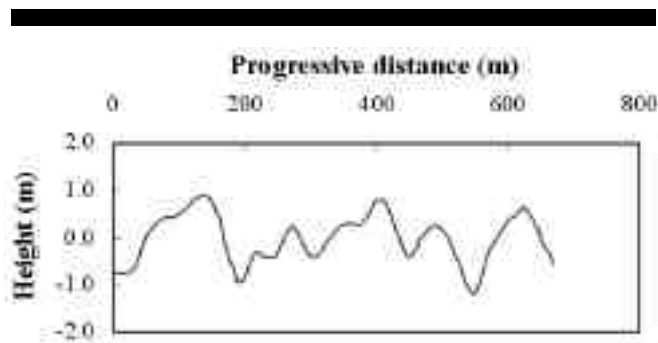


Figure 13. De-trended profile no. 3 in area no. 1.

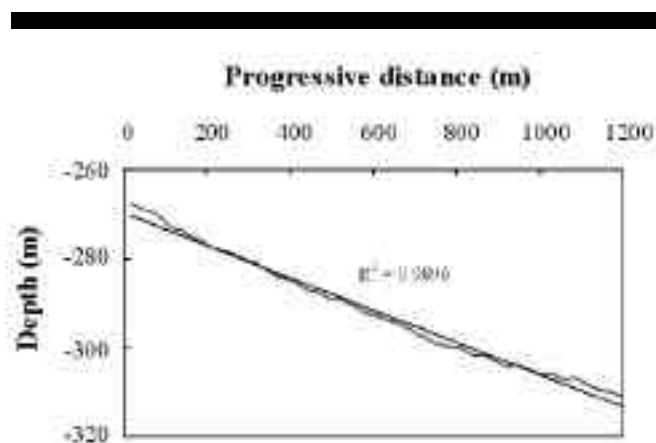


Figure 14. Profile no. 17 in area no. 3: original data and mean slope profile.

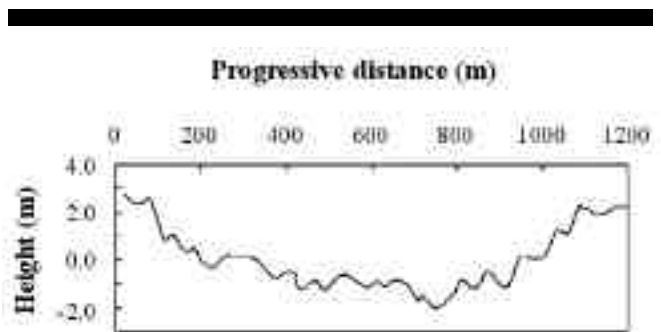


Figure 15. De-trended profile no. 17 in area no. 3.

Table II. Area no. 1: sand wave mean height and mean length for each depth class.

Depth (m)	Hm (m)	Lm (m)	S
200-210	0.92	88.42	0.010
210-220	1.59	120.68	0.013
220-230	1.29	104.45	0.012
230-240	1.15	132.14	0.009

Table III. Area no. 3: sand wave mean height and mean length for each depth class.

Depth (m)	Hm (m)	Lm (m)	S
260-270	0.84	64.96	0.013
270-280	0.95	91.58	0.010
280-290	1.24	106.41	0.012
290-300	1.78	113.92	0.016
300-310	1.23	173.38	0.007
310-320	1.16	107.63	0.011

DISCUSSION

Among the factors involved in bed-form generation and development, the correlation between height and wavelength is widely considered to be one of the most significant. Thus, a comparison was performed with the empirical relationship proposed by FLEMMING (2000) on the basis of 1491 couples of height/wavelength measures from flume studies, tidal current dominated shelf seas, ocean current dominated continental shelves, marginal seas experiencing episodic inflow events, large and small estuaries, rivers researches. In particular, as represented in Figure 16, there is a very poor matching between the present data and the relationship suggested by FLEMMING (2000). Indeed, the collected data are not well described by the exponential relationship $H = 0.0677L_{0.8098}$, corresponding to a linear log/log regression, even though to this law the author awards a universality nature because of the large range of plotted data ($H = 0.001 \div 20$ m, $L = 0.01 \div 1000$ m).

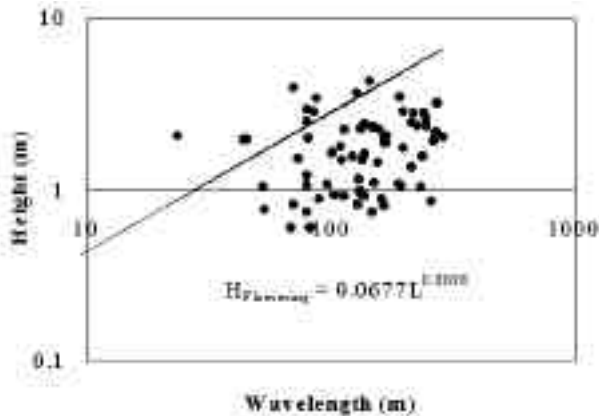


Figure 16. Comparison with FLEMMING (2000) law for the height/wavelength measures in both areas.

A comparison has also been performed with the theory of WERNER and KOCUREK (1997), according to which the evolution of bed-forms is strictly linked to the creation, migration, and destruction of the ends of their crests, i.e. of the defects. In particular, the time to evolve to a steady-state orientation for these sedimentary structures, which might be important in ocean engineering, has been determined.

This theory is based on the assumption that bed-form patterns reflect the dynamics of the defects in the patterns themselves. Indeed, the differential migration of defects within a field of bed-forms determines how crest line orientation responds to changing transport condition. It assumes that bed-form orientation can shift counterclockwise if the migration speed of the right-facing defect, called termination, exceeds that of the left-facing defect, i.e. the antitermination, and vice-versa.

The theory states that bed-forms achieve a steady-state orientation when the migration speed of terminations normal to their lines equals that of antiterminations, and that the rate of change of bed-form orientation is proportional to the number of defects per unit length of bed-form crest and to the difference between termination and antitermination migration speeds.

Assuming that the main part of a bed-form and its termination and antitermination are modelled as straight-line segments in plan view; given a vertically integrated sediment flux Q (volume per unit width per unit time) moving over a bed-form of height h_b , with Q inclined at angle α to the crest, the migration speed of the bed-form normal to the crest is:

$$v = \frac{Q \sin \alpha}{h_b} \quad (1)$$

Terminations and antiterminations, at angles T and T' , respectively, are taken to rotate around a hinge point at two

ends of a bed-form crest. Defect migration normal to the bed-form crest line is decomposed into motion normal to defect crest line and change in defect length.

Adopting the assumption that the duration of each transport event is sufficiently long that the defects point in the direction of transport over most of the event ($T = T' = 180^\circ$), the difference between termination and antitermination migration speeds over N different flux magnitudes Q_i , duration t_i , and transport directions α_i can be written

$$\Delta v_{\perp} = - \sum_{i=1}^N \frac{Q_i \Delta t_i}{hT} 2 \cos \alpha_i \sin \alpha_i \quad (2)$$

$$T = \sum_{i=1}^N \Delta t_i \quad (3)$$

Since migration speed of defects can be predicted, the time to evolve to a steady-state orientation after a change in transport direction can be estimated.

WERNER and KOCUREK (1997) conclude that the predicted rate of change in mean bed-form orientation is

$$\frac{d\alpha_{\perp}}{dt} = -\rho \Delta v \quad (4)$$

where $\rho = 1/\bar{l}$ is the number of defect pairs per unit length of crest and \bar{l} is the average length of bed-form crests.

This theory, here briefly summarized, was applied to sand waves located in areas no. 1 and no. 3. It is worth pointing out that, since sand waves in the Messina Strait are mainly due to tide, the flow has a complex three dimensional structure which influences the bed-forms, (highly 3D in nature), as also described in a different context (i.e. for small scale bed-forms) by ROOS and BLONDEAUX (2001).

However a rough analysis can be performed, by considering only the main component of the flow.

For area no. 1, such a component can be determined on the basis of the following considerations. Since measured available data represented in Figures 4 and 5 were taken 3 m over the bottom, which is characterized by sandy gravel sediments, if we assume a logarithmic profile for the velocity, currents able to mobilize sediments (i.e. which exceed the value 0.4 of the Shields' parameter) are those stronger than 0.8 m/s. It implies that for area no.1, bottom morphology is influenced only by currents characterized by an angle of $\sim 0^\circ$ with respect to the north direction.

On the basis of a similar analysis, in area no. 3, which is characterized by a sandy bottom, only currents higher than 0.7 m/s can be considered, that is, currents characterized by a direction of $\sim 330^\circ$ with respect to the north direction.

As the direction orthogonal to sand wave crests in area no. 1 is characterized by an angle of $\sim 300^\circ$ with respect to the north direction, the angle between this direction and the main component of the flow is $\sim 60^\circ$ (see Figure no. 17).

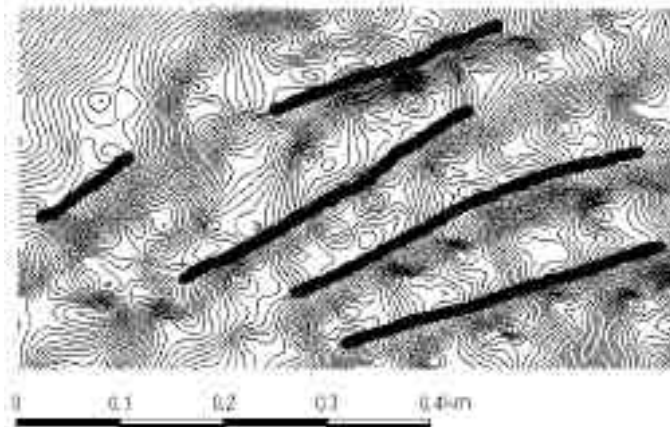


Figure 17. Area no.1: sand wave crest orientation and length.

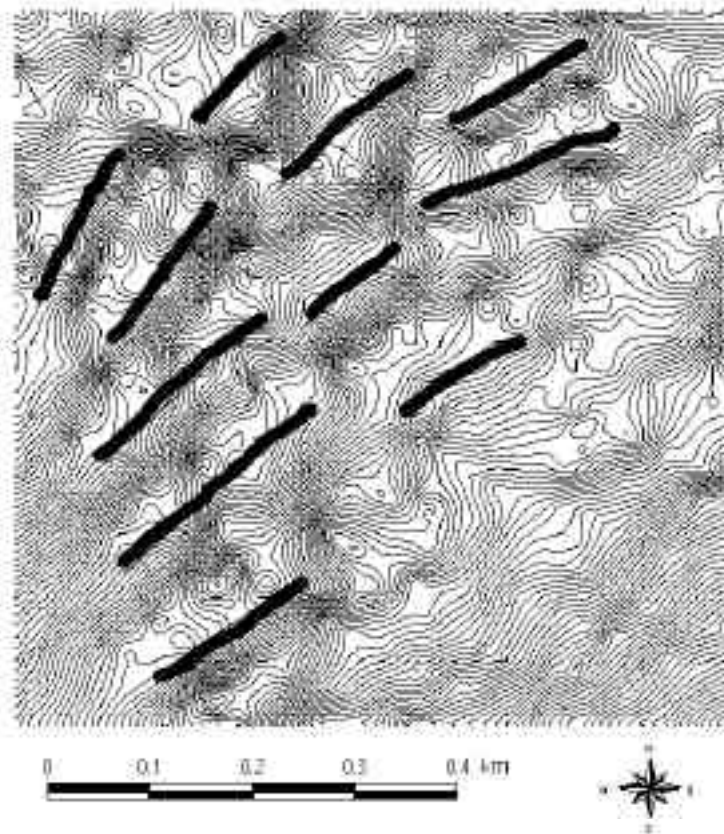


Figure 18. Area no.3: sand wave crest orientation and length

Migration rate v can be set equal to 1 m/year on the basis of previously mentioned qualitative observations of a partially floating pipeline between two successive sand wave crests.

Since the average length of sand wave crests in area no. 1 is 365 m, integrating equation (4), the expected time for the sand wave reorientation from their present misalignment is 430 years.

In area no. 3, the direction orthogonal to sand wave crests is characterized by an angle of $\sim 335^\circ$ with respect to the north direction, so the angle with the main component of the flow is $\sim 5^\circ$ and the mean length of sand wave crests is 170 m. Integrating equation (4) the expected time for sand wave reorientation from their present misalignment is 110 years.

CONCLUSIONS

An analysis on sand wave characteristics as observed in two different areas in the Messina Strait was performed on the basis of bathimetric data gathered during two surveys carried out in 1991 and 1992 respectively. The study was also based on information concerning both the sedimentology and the hydrodynamics in the Strait.

As a matter of fact, these sedimentary structures are made up with rather coarse sand. Therefore, even though tidal conditions are different in the two areas, one area being characterised by a very narrow tidal ellipse, only the highest currents are able to mobilise sediment and, in turn, to influence bottom morphology. A morphometric analysis showed that, although in both areas wavelength ranges between 50 and 300 m, while height ranges between 0.5 and 3.5 m, there is not a remarkable variability of these geometric characteristics at constant depth; indeed the maximum scatters between class average and total average values of H_m and L_m are 28% and 26% respectively in one area, while they are 48% and 58% respectively in the other one. As regard to steepness, it appears always close to 0.01, thus suggesting a likely negligible effect of flow separation on these sand wave morphodynamics.

As the correlation between height and wavelength is widely considered to be one of the most important factors involved in bed-form generation and development, a comparison was made between the present data and the relationship proposed by FLEMMING (2000), but it gave a quite poor matching.

Time for the examined bed-forms to re-orient has finally been computed on the basis of WERNER and KOCUREK (1997) defect dynamics theory. Such time has been estimated as more than one century for both areas, suggesting that it does not play a significant role on problems concerning duct and cable cross design.

Major attention on migration speed is then suggested, which, although playing a crucial role, has never been assessed in specific studies.

ACKNOWLEDGMENTS

This work has been carried out in the framework of PRIN Cofin2000 "Idrodinamica e morfodinamica di ambienti a marea" founded by MIUR (contract no. 20104030020). SNAMPROGETTI, ENI and SOCIETA' STRETTO DI MESSINAS.p.A. are gratefully acknowledged for allowing data from different surveys to be published. Many thanks are due to Dr. M. Drago, Dr. L. Jovenitti and Dr. E. Vullo for suggestions and for discussions arisen from the work.

LITERATURE CITED

- BLONDEAUX, P., BROCCINI, M., DRAGO, M., IOVENITTI, L., and VITTORI, G., 1999. Sand waves formation: preliminary comparison between theoretical predictions and field data. *Proc. I.A.H.R. Symposium on River, Coastal and Estuarine Morphodynamics*, Genova, 1, 197-206.
- COLANTONI, P., 1987. Marine geology of the Strait of Messina. In: *Le Déroit de Messine (Italie). Evolution tectono-sédimentaire récente (pliocène et quaternaire) et environnement actuel. Doc. et trav. IGAL*, Paris, 11, 272, 191-209.
- COLANTONI, P., 1995. Seafloor morphology and sediment dynamics in the Strait of Messina. In: GUGLIELMO L., MANGANARO A. and DE DOMENICO (eds.), *The Strait of Messina Ecosystem*. Proceedings of the Symposium held in Messina 4-6 April 1991, 83-94.
- FLEMMING, B. W., 2000. The role of grain size, water depth and flow velocity as scaling factors controlling the size of subaqueous dunes. In: ALAIN TRENTESAUX and THIERRY GARLAN (eds.), *Marine Sandwave Dynamics*, Lille, France, 23-24 March.
- FREDSØE, J., and DEIGAARD, R., 1993. Mechanics of coastal sediment transport. *World Scientific*, 3, 260-289.
- GERKEMA, T., 2000. A linear stability analysis of tidally generated sand waves. *Journal of Fluid Mechanics*, 417, 303-322.
- HULSCHER, S.J.M.H., 1996. Tidal-induced large scale regular bed-form patterns in three-dimensional shallow water model. *Journal of Geophysical Research*, 101, C9, 20727-20744
- HUTHENANCE, J., 1982. On the formation of sandbanks of finite extent. *Est. Coast. Shelf Sci.*, 15, 277-299.
- MONTENAT, C., BARRIER, P., and DI GERONIMO, I., 1987. The Strait of Messina, past and present: a review. *Le déroit de Messine (Italie). Evolution tectono-sédimentaire récente (pliocène et quaternaire) et environnement actuel. Doc. et trav. IGAL*, Paris, 11, 272, 7-13.
- MOSETTI, F., 1988. Some news on the currents in the Strait of Messina. *Bollettino di Oceanologia Teorica ed Applicata*, VI, 3, 119-201.
- NESTEROFF, W. D., and RAWSON, M., 1987. Dynamics of modern sediments in the Strait of Messina (Sicily) and south-west of Calabria. *Le déroit de Messine (Italie). Evolution tectono-sédimentaire récente (pliocène et quaternaire) et environnement actuel. Doc. et trav. IGAL*, Paris, 11, 272, 211-223.
- ROOS, P. C., and BLONDEAUX, P., 2001. Sand ripples under sea waves. Part 4. Tile ripple formation. *J. Fluid Mech.*, 447, 227-246.

- SELLI, R.; COLANTONI, P.; FABBRI A., ROSSI S., BORSETTI, A. M., and GALLIGNANI, P., 1979. Marine geological investigation on the Messina Strait and its approaches. *Giornale di Geologia*, serie 2, XLII, 2, 1-70.
- TOMASIN, A., and TOMASINO, M., 1980. Correnti e livelli marini nello Stretto di Messina: nuovi contributi di misure ed elaborazioni. *Proc. 4° Congresso A.I.O.L.* Chiavari, 10-1, 10-9.
- VERCELLI, F., 1925. Il regime delle correnti e delle maree nello Stretto di Messina. *Commissione Internazionale del Mediterraneo*.
- WERNER, B.T., 1999. Complexity in Natural Landform Patterns. *Science*, 284, 102-104.
- WERNER, B.T., and KOCUREK, G., 1997. Bed-form dynamics: Does the tail wag the dog? *Geology*, 29, 9, 771-774.